Article

Journal of Vibration and Control
2018, Vol. 24(1) 110–125

DOI: 10.1177/1077546316634562
journals.sagepub.com/home/jvc
SAGE

# Load frequency control of a two-area multi-source power system using a tilt integral derivative controller

**Pretty Neelam Topno and Saurabh Chanana**

**Abstract**

This paper introduces a tilt integral derivative controller as the supplementary controller for load frequency control of a two-area interconnected power system. The optimal value of parameters of the tilt integral derivative controller is evaluated using constrained nonlinear optimization by means of a performance index-based method. The proposed tilt integral derivative control offers superior properties such as simple parameter tuning and its performance does not compromise the occurrence of any parameter variations in the system. To verify these features of the controller, the test system is subjected to step load disturbance and parameter variations that ensure the robustness of the tilt integral derivative controller. Comparative analysis with previously published work indicates that the proposed tilt integral derivative controller gives better performance and holds the property of robustness. Simulations have been performed using Matlab®.

**Keywords**

Interior point algorithm, load frequency control, proportional integral derivative control, power system, tilt integral derivative control

## 1. Introduction

In a large interconnected power system, transient disturbances promote instabilities in the system. These instabilities cause imbalance between load and generation, affecting the normal operation of the power system. To keep this balance, the prime mover governing system helps to control the system frequency and schedule tie-line flow. This action is called load frequency control (LFC) or automatic generation control (AGC) (Elgerd, 1982; Kundur, 1994). LFC plays an important role in normal operating conditions as well as during transient disturbances. The main objectives of LFC are as follows:

a. to maintain zero steady-state error during operation;
b. to maintain system frequency under permissible limits;
c. to maintain equal load distribution on neighboring units;
d. to control power flow between interconnected control areas.

All these objectives are required to be achieved for the smooth operation of any interconnected power system. The LFC problem constitutes control of frequency and power flow between interconnected control units. Many control theories and methods such as classical control (Concordia and Kirchmayer, 1953; Van Ness, 1963; Cohn, 1967), modern control (Fosha and Elgerd, 1970; Pan and Liaw, 1989; Aldeen and Marah, 1991; Gozde and Taplamacioglu, 2011; Zribi et al., 2005), intelligent control (Indulkar and Raj, 1995; Ghoshal, 2004; Pothiya et al., 2006; Soundarrajan and Sumathi, 2011) and sliding mode control (Kumar et al., 1985; Ai-Hamouz and

Department of Electrical Engineering, NIT Kurukshetra, India

Received: 5 May 2015; accepted: 19 January 2016

**Corresponding author:**
Pretty Neelam Topno, Department of Electrical Engineering, NIT Kurukshetra, India.
Email: pretty.topno@gmail.com

Abdel-Magid, 1993) have been reported in the literature. In addition, several optimization techniques such as evolutionary computation techniques (Rerkpreedapong et al., 2003; Shayeghi et al., 2007; Roy et al., 2010; Soundarrajan et al., 2012) have been developed to obtain optimal values of controller parameters. As the interconnected power system undergoes several changes such as increased share of renewable energy (Doolla and Bhatti, 2007; Verma and Kumar, 2012; Rangaswami and Sennappan, 2013) and multiple source of power generation (Ramakrishna and Bhatti, 2008; Parmar et al., 2012; Barisal, 2015), complexity in the structure as well as operation has also been increased. The rise in complexity allows new techniques and algorithms to be examined for LFC problem. Nowadays, a concept of noninteger or fractional order controller (FOC) is gaining the attention of researchers working in the area of control system. FOC is based on fractional calculus, which can be defined as the generalization of classical calculus to orders of integration and differentiation not necessarily integer. There are four representative FOCs in the literature, namely, TID (tilted integral derivative) controller, CRONE controller (*Contrôle Robuste d'Ordre Non Entier*), proportional integral derivative (PID) controller and fractional lead-lag compensator (Xue and Chen, 2002). The traces of fractional order controller can be found in different area of control engineering (Podlubny, 1996; Xue et al., 2006). The effects of fractional order PID (FOPID) control wwere first taken into account in the LFC problem by Alomoush (2010). Moreover, the application FOPID controller in power system control has been reported (Taher et al., 2010; Debbarma et al., 2013; Sondhi and Hote, 2014). However, none of the FOCs other than FOPID has been proposed in the LFC problem.

In this paper, the TID controller has been proposed as a LFC in an interconnected power system. The optimal values of controller parameters are obtained using an appropriate optimization technique. The approach begins by formulating a minimization function using an integral time absolute error (ITAE) index, resulting into a constrained nonlinear optimization problem. Thereafter, the optimization problem is solved using interior point algorithm to obtain the optimum values of controller parameters. The main objective of this study is to evaluate the capability of TID controller as a better controller by using the constrained nonlinear optimization technique. As a result, the TID controller improves the stability and response of a system and shows better performance than PID controller (Barisal, 2015).

## 2. System investigated

The AGC model on which the investigation has been carried out is a multi-source identical two-area thermal system with high-voltage direct current high-voltage direct current (HVDC). Each area in the model is provided with a thermal unit, hydro unit, and gas unit in which each unit is comprises a governor, a reheat thermal turbine in a thermal unit, a hydro turbine in a hydro unit and a gas turbine in a gas unit. The two areas are connected through a tie line, which allows the flow of electric power among the interconnected areas. The control unit monitors the system frequency and tie-line power deviation, and tries to restore the normal operating state of the system during unfavorable conditions such as load perturbations. The block diagram model of the two-area thermal system is shown in Figure 1.

For a two-area system, the area control error $ACE_1$ and $ACE_2$ is given by

$$ACE_1 = B_1\Delta f_1 + \Delta P_{\text{tie1}} \quad (1)$$

$$ACE_2 = B_2\Delta f_2 - \Delta P_{\text{tie2}} \quad (2)$$

And $\Delta P_{\text{tie},1,2}$ is the tie-line power flow error between area-1 and area-2. The frequency bias coefficient $B_1$ and $B_2$ is given by

$$B_1 = \frac{1}{R_1} + D_1 \quad (3)$$

$$B_2 = \frac{1}{R_2} + D_2 \quad (4)$$

## 3. TID controller

Tilt integral derivative control is a feedback control that is similar to PID control and also possesses the merits of PID control; the proportional action of PID control is replaced by a tilted proportional action in TID control, having a transfer function $1/s^{(1/n)}$ or $s^{-1/n}$. The tilt effect of the controller provides a feedback gain as a function of frequency, which is tilted with respect to the gain/frequency of a conventional compensator. So, the entire compensator is referred to as a TID compensator. The structure of the TID control is shown in Figure 2.

The mathematical description of the transfer function $G_{\text{TID}}(s,\beta)$ is

$$G_{\text{TID}}(s,\beta) = \frac{T}{s^{\frac{1}{n}}} + \frac{I}{s} + Ds \quad (5)$$

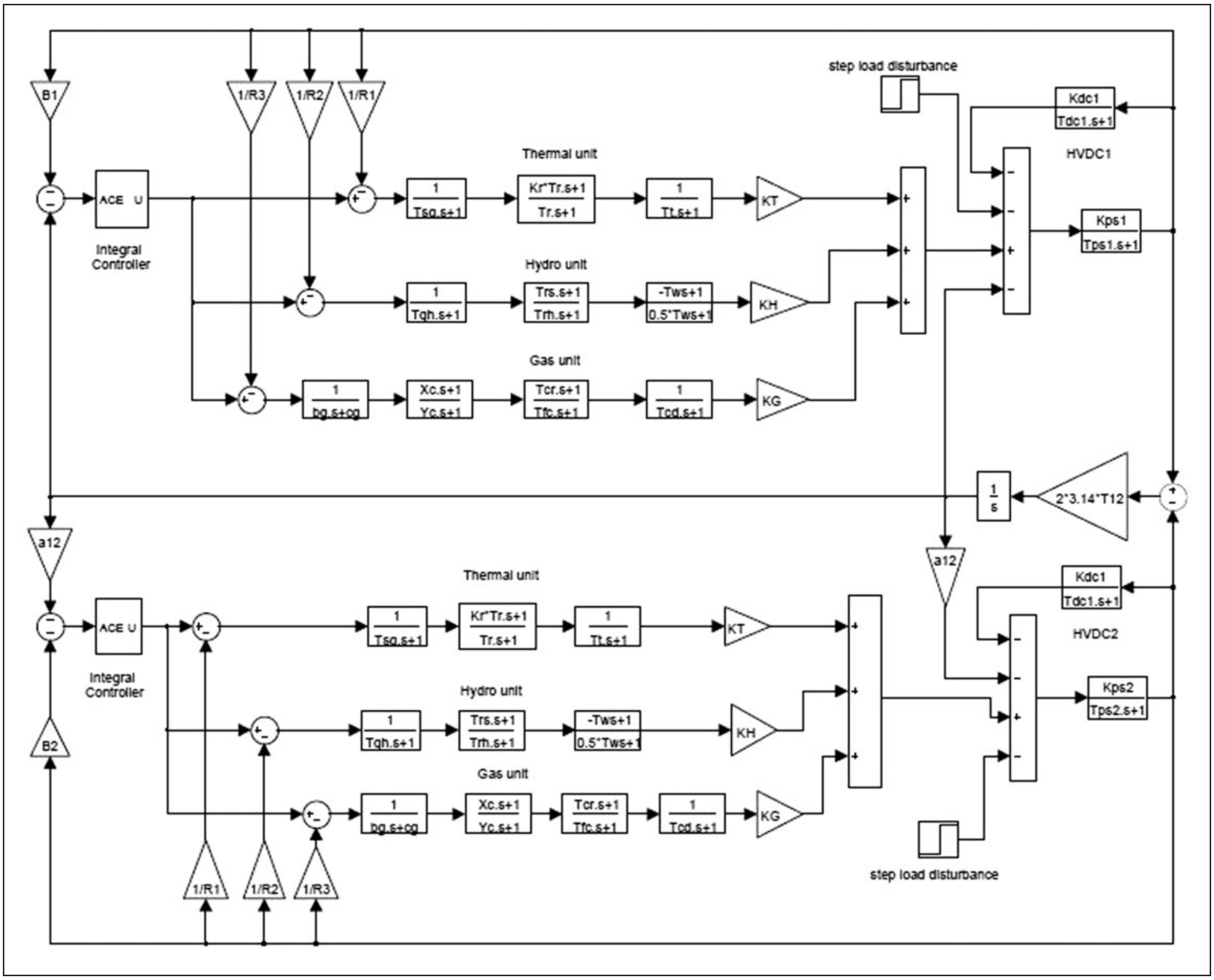


**Figure 1.** Block diagram model of multi-source multi-area power system.

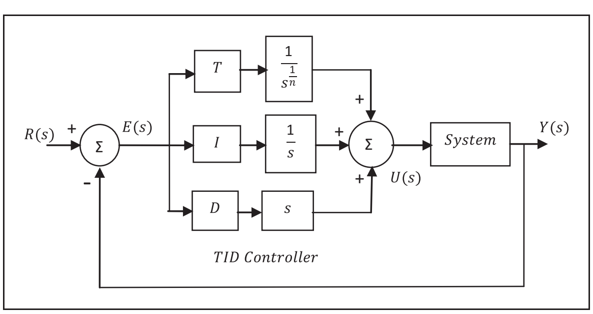


**Figure 2.** Structure of tilt integral derivative (TID) controller in a closed loop system.

where $G_{\mathrm{TID}}(s, \beta)$ is the transfer function of TID controller, is a complex variable $s \in C$ and is parameterized by $\beta \in \mathbb{R}^4$, where $\beta = \begin{bmatrix} T & I & D & n \end{bmatrix}^{\mathrm{T}} \in \mathbb{R}^4$. The four control parameters are $T, I, D$ and $n$ with $n \in \mathbb{R}$ $n \neq 0$. The range of $n$ is preferably between two and three. The resulting transfer function of the entire compensator more closely approximates an optimal transfer function, thereby achieving improved feedback controller. Further, as compared to conventional PID compensators, the TID compensator allows for simpler tuning, better disturbance rejection ratio, and smaller effects of plant parameter variations on closed loop response (Lurie, 1994). In this paper, two properties of the TID controller are been discussed. One is the property of simple and easy tuning. Second is the insignificant effect of parameter variations on the TID controller in which, regardless of parameter uncertainty, the performance of the TID controller remains unaffected.

## 4. Optimization of controller parameters

In this paper, the notion of performance index is used to design an optimal control system for an AGC model. The approach progresses when an error function is formulated into an objective function later to be minimized by using an appropriate optimization technique (Kywang and El-Sharkawi, 2008). In control system design, there are four performance indices: integral of square error (ISE), integral of absolute value of error (IAE), integral of time multiplied by squared error (ITSE) and integral of time multiplied by absolute error (ITAE). The performance index considered for this study is ITAE, given by

$$J = ITAE = \int_{0}^{t_{\text{sim}}} t \cdot \left(\left|\Delta f_1(t)\right| + \left|\Delta f_2(t)\right| + |\Delta P_{\text{Tie}}|\right) \cdot \mathrm{d}t \tag{6}$$

In equation (6), the objective function $J$ is required to be minimum, which involves the process of optimization. The optimization process involves minimizing of an objective function by imposing a set of constraints on the function while evaluating the value of objective function. This yields an optimization problem and in this case it is a constrained optimization problem given by

$$\begin{aligned} &\text{Minimize}\, f(x) \\ &\text{Subjectto}\ h(x) = 0, g(x) \leq 0 \end{aligned} \tag{7}$$

where $f : R^n \rightarrow R, h : R^n \rightarrow R^t, g : R^n \rightarrow R^m$ are smooth functions (Byrd et al., 1999).

However, in this study, the minimization of the objective function $J$ of a two-area system is dependent on the controller parameters. Therefore, the optimal value of controller parameters is required to be determined.

In this paper, an identical two-area system is considered, which reflects identical controllers in both areas. Therefore, the optimal values of TID controller constants $(T, I, D, n)$ are obtained by solving the optimization problem formulated while imposing the restriction on the controller parameters. The constrained optimization problem for a two-area system is given by

$$\begin{aligned} &\text{Minimize}\,(J) \\ &\text{subjectto} \\ &T_{\text{min}} \leq T \leq T_{\text{max}} \\ &I_{\text{min}} \leq I \leq I_{\text{max}} \\ &D_{\text{min}} \leq D \leq D_{\text{max}} \\ &n_{\text{min}} \leq n \leq n_{\text{max}} \end{aligned} \tag{8}$$

where the subscripts 'min' and 'max' denote minimum bound and maximum bound, respectively. The approximate range of controller parameters has been set firstly using simple PID tuning techniques and then this approximate range is used as bounds to the constrained optimization problem. Equation (8) is a constrained optimization problem solved using the interior-point algorithm. The algorithm attempts to find a constrained minimum of a scalar function of several variables starting at an initial estimate. The advantage of using interior point algorithm over other algorithms is that it always satisfies bound constraints in all intermediate iterations. Mathematically, the problem formulated is of the form

$$\begin{aligned} &\underset{\beta \in \mathbb{R}^4}{\arg\min} \left\{ (J) - \mu \sum_{k=1}^{8} \ln x_{1k} \right\} \\ &\text{Subject to } g(\beta, q) + x_1 = 0 \end{aligned} \tag{9}$$

where $q = [T_{\text{min}} \quad T_{\text{max}} \quad I_{\text{min}} \quad I_{\text{max}} \quad D_{\text{min}} \quad D_{\text{max}} \; n_{\text{min}} \; n_{\text{max}}]^{\text{T}} \in \mathbb{R}^8$ is the bound parameter vector for the TID controller, $x_1 = [x_{11} \quad x_{12} \quad x_{13} \quad x_{14} \quad x_{15} \quad x_{16} \quad x_{17} \quad x_{18}]^{\text{T}} \in \mathbb{R}^8$ is the slack variable vector and $g(\beta, q)$ is the matrix valued constrained function. In equation (9), $\mu > 0$ is the barrier parameter, and the slack variable $x_1$ is assumed to be positive. To determine the unconstrained solution of equation (9), the Lagrangian function is defined as

$$L_{\text{TID}}(\beta, x_1, \lambda_g) = (J) - \mu \sum_{k=1}^{8} \ln x_1 k + \lambda_g^{\text{T}}(g(\beta, q) + x_1) \tag{10}$$

where $\lambda_g \in \mathbb{R}^8$ is the Lagrange multiplier and equation (10) is the required unconstrained function to optimally evaluate the parameters of respective controllers with respect to first-order optimality conditions. Detailed information regarding the numerical solution of optimality conditions can be found in Byrd et al. (1999) and Waltz et al. (2006).

## 5. Result and analysis

A multi-source multi-area power system with HVDC link has been considered for the studies, the parameters of which are given by Barisal (2015) and are presented in the Appendix. The minimum and maximum bound of the gain parameters $(T, I, D)$ are 0 and 10, respectively, but the bounds of parameter $n$ are chosen to be 2 as $n_{\text{min}}$ and 3 as $n_{\text{max}}$. Here, a TID controller is proposed as a load frequency controller for a multi-source multi-area system considering normal operating conditions and parameter uncertainty. The performance of the proposed TID controller is compared with the PID controller (Barisal, 2015).

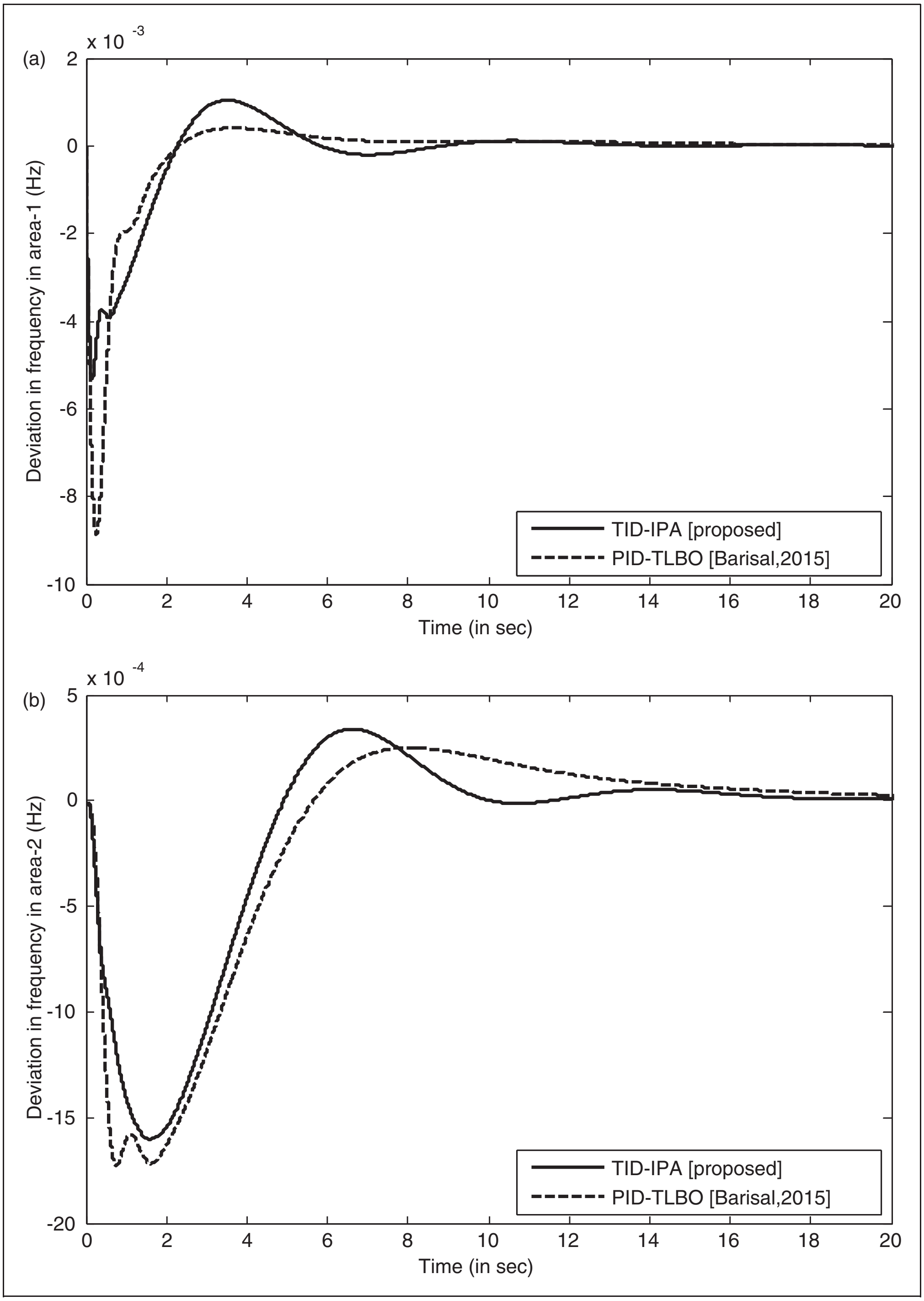


**Figure 3.** (a) Frequency deviation in area-1 at nominal value of system parameters. (b) Frequency deviation in area-2 at nominal value of system parameters. (c) Tie-line power deviation at nominal value of system parameters. Tilt Integral Derivative Control using Interior Point Algorithm (TID-IPA), Proportional Integral Derivative Control using Teaching Learning based Optimization (PID-TLBO).

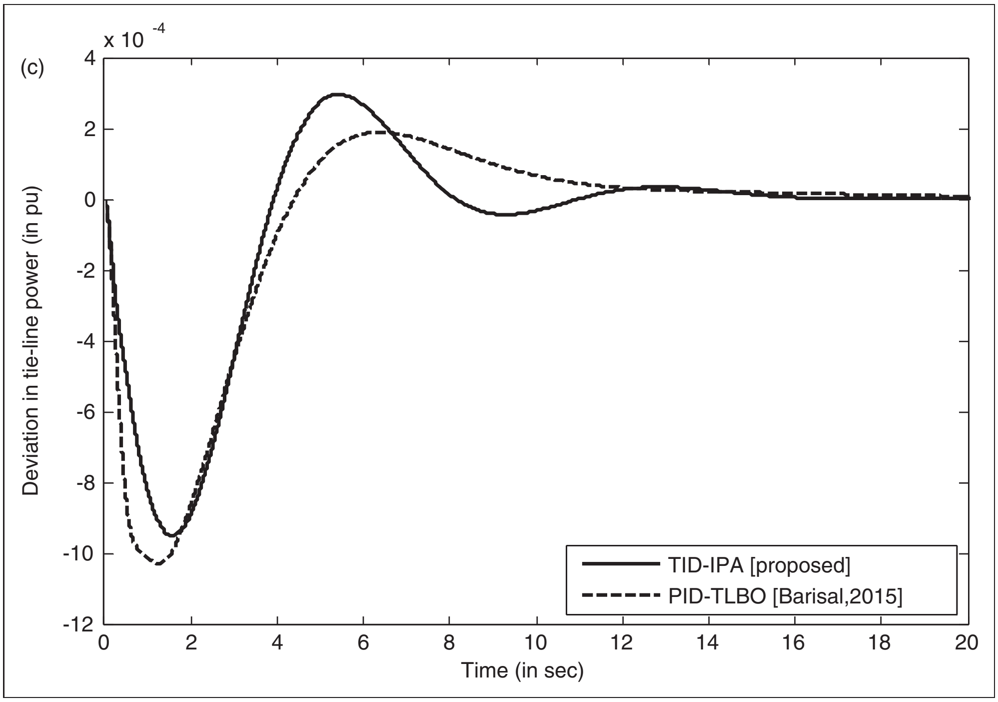


**Figure 3.** Continued.

## *5.1. At normal operating conditions*

When area-1 is subjected to step load variation of 0.01 pu under nominal value of system parameters, the frequency deviation in area-1, frequency deviation in area-2 and tie-line power deviation is shown in Figure 3(a), Figure 3(b) and Figure 3(c), respectively. The optimal values of TID controller parameters under step load variation of 0.01 pu are given by

For Thermal unit : $\mathrm{T}_{TH} = 5.5726$, $\mathrm{I}_{TH} = 3.9653$, $\mathrm{D}_{TH} = 9.9621$, $\mathrm{n}_{TH} = 2.5405$,
For Hydro Unit : $\mathrm{T}_{HY} = 0.7051$, $\mathrm{I}_{HY} = 0.0354$, $\mathrm{D}_{HY} = 0.0394$, $\mathrm{n}_{HY} = 2.5405$.
For Gas Unit : $\mathrm{T}_{GAS} = 8.7211$, $\mathrm{I}_{GAS} = 7.4725$, $\mathrm{D}_{GAS} = 2.4185$, $\mathrm{n}_{GAS} = 2.5405$.

## *5.2. Effect of parameters variation*

Parameters of the system such as frequency bias factor, time constant of turbine, operating load condition and synchronizing co-efficient are subjected to a variation of ±25% and ±50% from their nominal value and the system response (for 25% and 50% increase and 25% and 50% decrease) is obtained using the same value of controller parameter as used for normal operating conditions.

a. 25% increase in system parameters with respect to nominal values
The frequency deviation in area-1 with respect to 25% increase in frequency bias factor $B$, time constant of turbine $T_t$, operating load condition of area-1 $P_{d1}$ and synchronizing co-efficient $T_{12}$ from their nominal value are shown in Figure 4(a), 4(b), 4(c) and 4(d), respectively.
b. 25% decrease in system parameters with respect to nominal values
The frequency deviation in area-1 with respect to 25% decrease in frequency bias factor $B$, time constant of turbine $T_t$, operating load condition of area-1 $P_{d1}$ and synchronizing co-efficient $T_{12}$ from their nominal value are shown in Figure 5(a), 5(b), 5(c) and 5(d), respectively.
c. 50% increase in system parameters with respect to nominal values
The frequency deviation in area-1 with respect to 50% increase in frequency bias factor $B$, time constant of turbine $T_t$, operating load condition of area-1 $P_{d1}$ and synchronizing co-efficient $T_{12}$ from their nominal value are shown in Figure 6(a), 6(b), 6(c) and 6(d), respectively.
d. 50% decrease in system parameters with respect to nominal values
The frequency deviation in area-1 with respect to 50% decrease in frequency bias factor $B$, time constant of turbine $T_t$, operating load condition of area-1 $P_{d1}$ and synchronizing co-efficient $T_{12}$ from

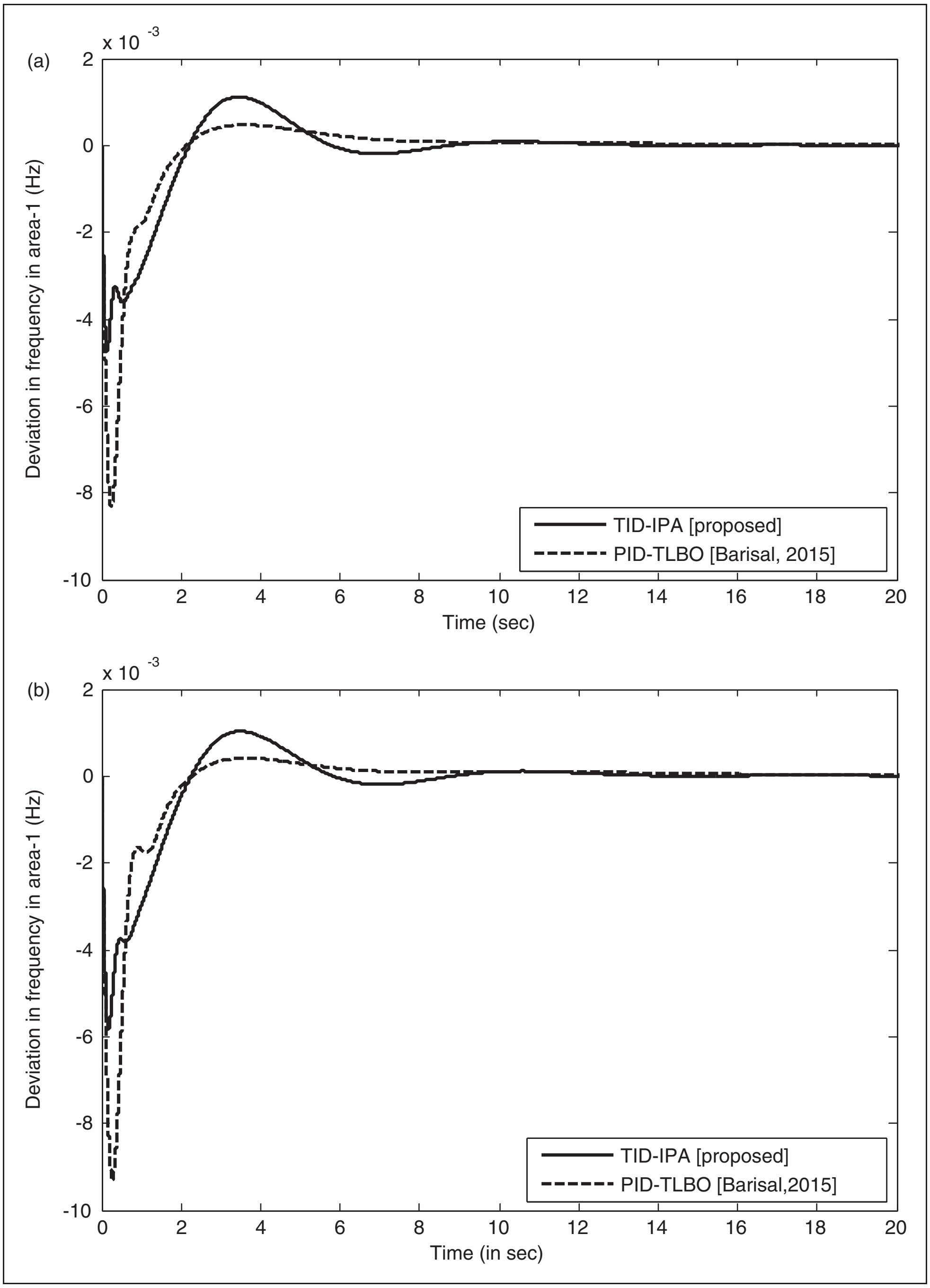


**Figure 4.** (a) Frequency deviation in area-1 due to 25% increase in frequency bias factor. (b) Frequency deviation in area-1 due to 25% increase in constant of turbine. (c) Frequency deviation in area-1 due to 25% increase in operating load condition. (d) Frequency deviation in area-1 due to 25% increase in synchronizing co-efficient. Tilt Integral Derivative Control using Interior Point Algorithm (TID-IPA), Proportional Integral Derivative Control using Teaching Learning Based Optimization (PID-TLBO).

their nominal value are shown in Figure 7(a), 7(b), 7(c) and 7(d), respectively.

For the cases discussed, i.e. normal operating condition and under the effect of parameter variation, the system performance is finally analyzed by evaluating settling time (in seconds) and overshoot (in per unit) of system response based on the 2% of final value, presented in Table 1.

As the calculated settling time has been qualified for the designated tolerance band, i.e. 2% of final value, it is said that the response has been settled at zero seconds. However, the overshoot of the system response is obtained, which shows that the TID controller shows

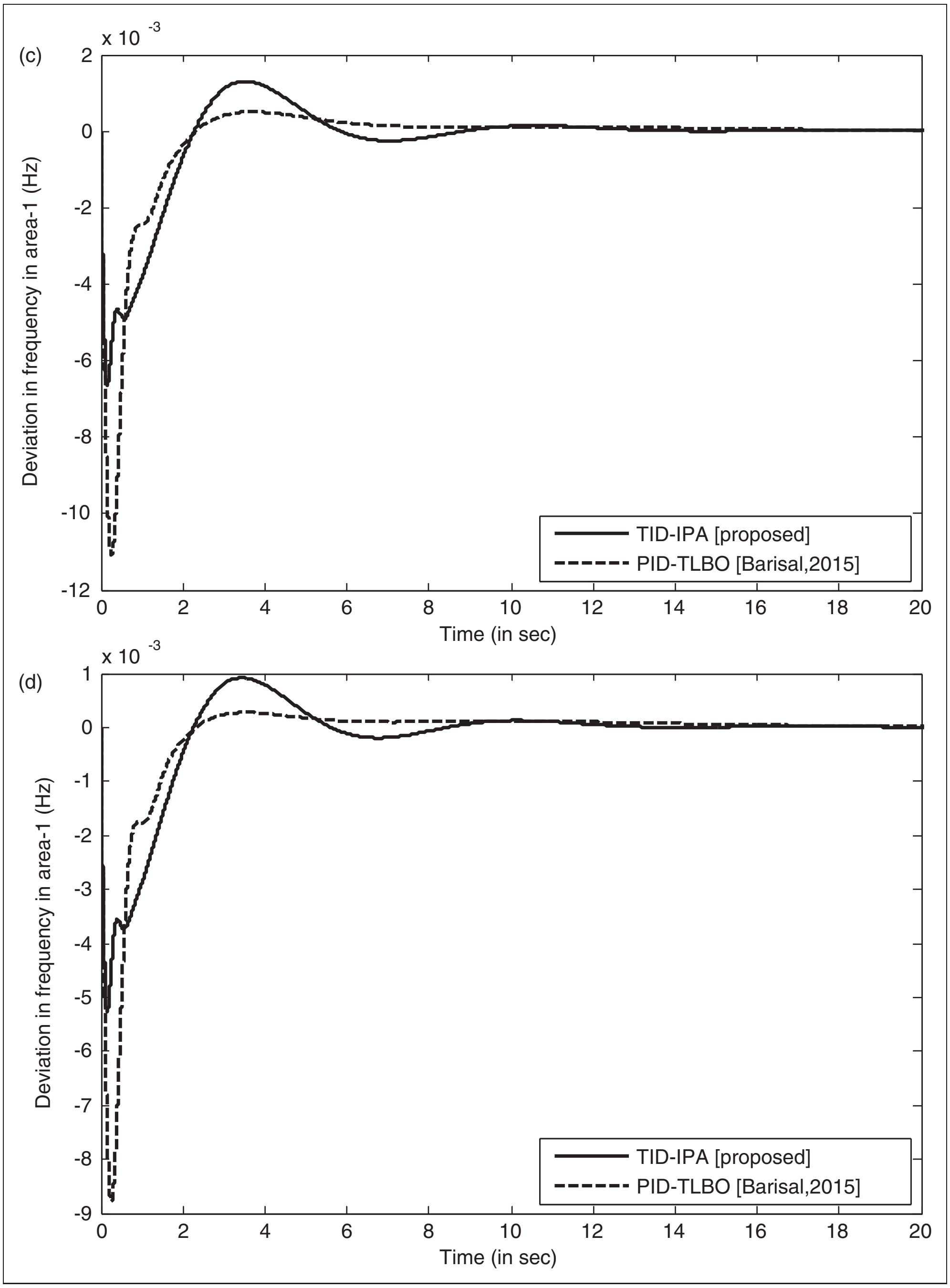


**Figure 4.** Continued.

more robustness. In addition, the value of the objective function obtained through different performance indices has been presented in Table 2.

The study of the effect of parameter variation shows that, regardless of parameter uncertainty, the performance of the TID controller remains unaffected and offers a better system response in comparison to the PID controller (Barisal, 2015).

## 6. Conclusion

In this paper, a tilt integral derivative controller (TID) has been implemented on a two-area thermal system. The optimal value of proposed TID controller parameters was obtained using a constrained nonlinear optimization technique. The comparison of dynamic responses for different controllers is carried out,

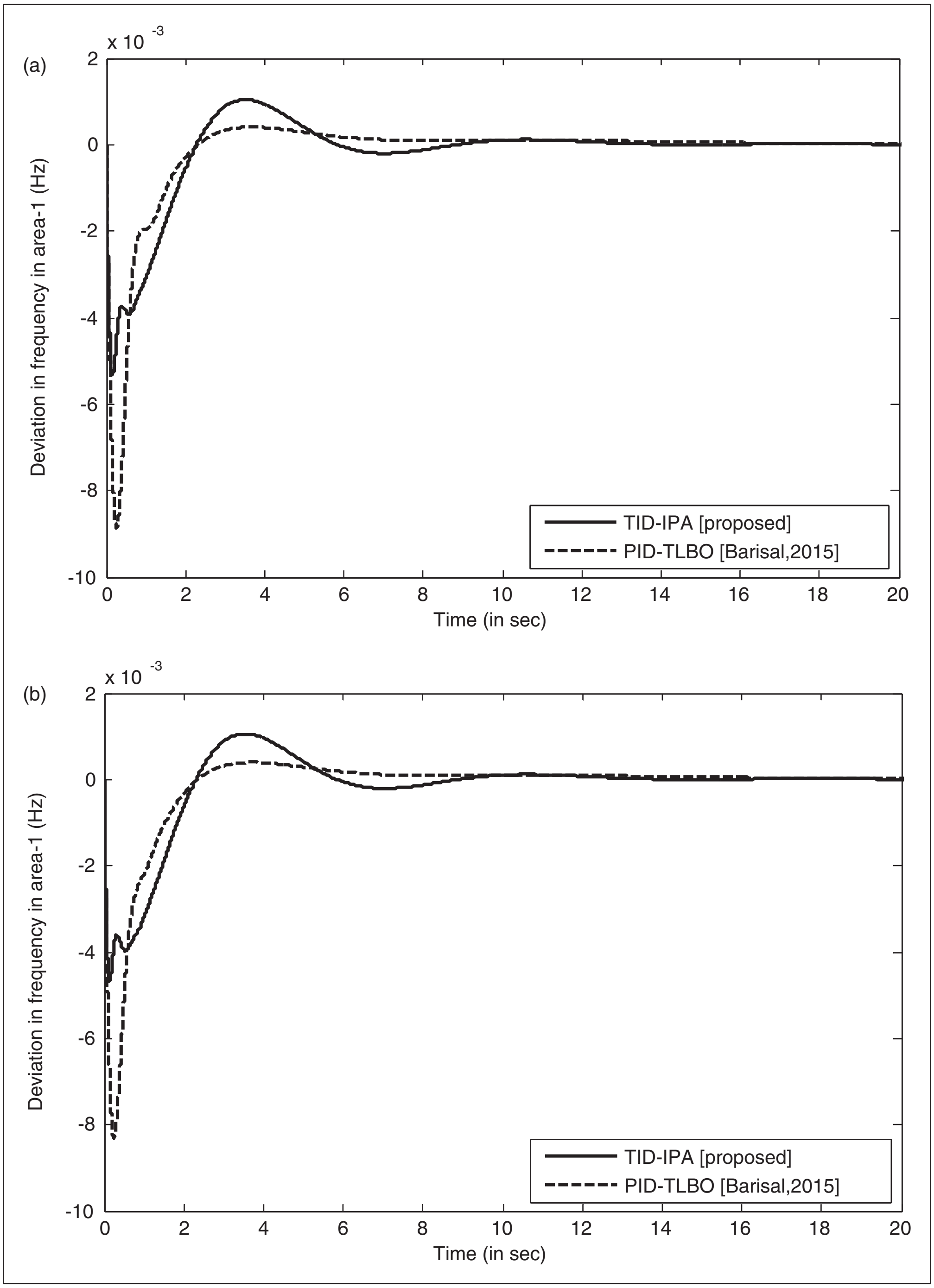


**Figure 5.** (a) Frequency deviation in area-1 due to 25% decrease in frequency bias factor. (b) Frequency deviation in area-1 due to 25% decrease in constant of turbine. (c) Frequency deviation in area-1 due to 25% decrease in operating load condition. (d) Frequency deviation in area-1 due to 25% decrease in synchronizing co-efficient. Tilt Integral Derivative Control using Interior Point Algorithm (TID-IPA), Proportional Integral Derivative Control using Teaching Learning based Optimization (PID-TLBO).

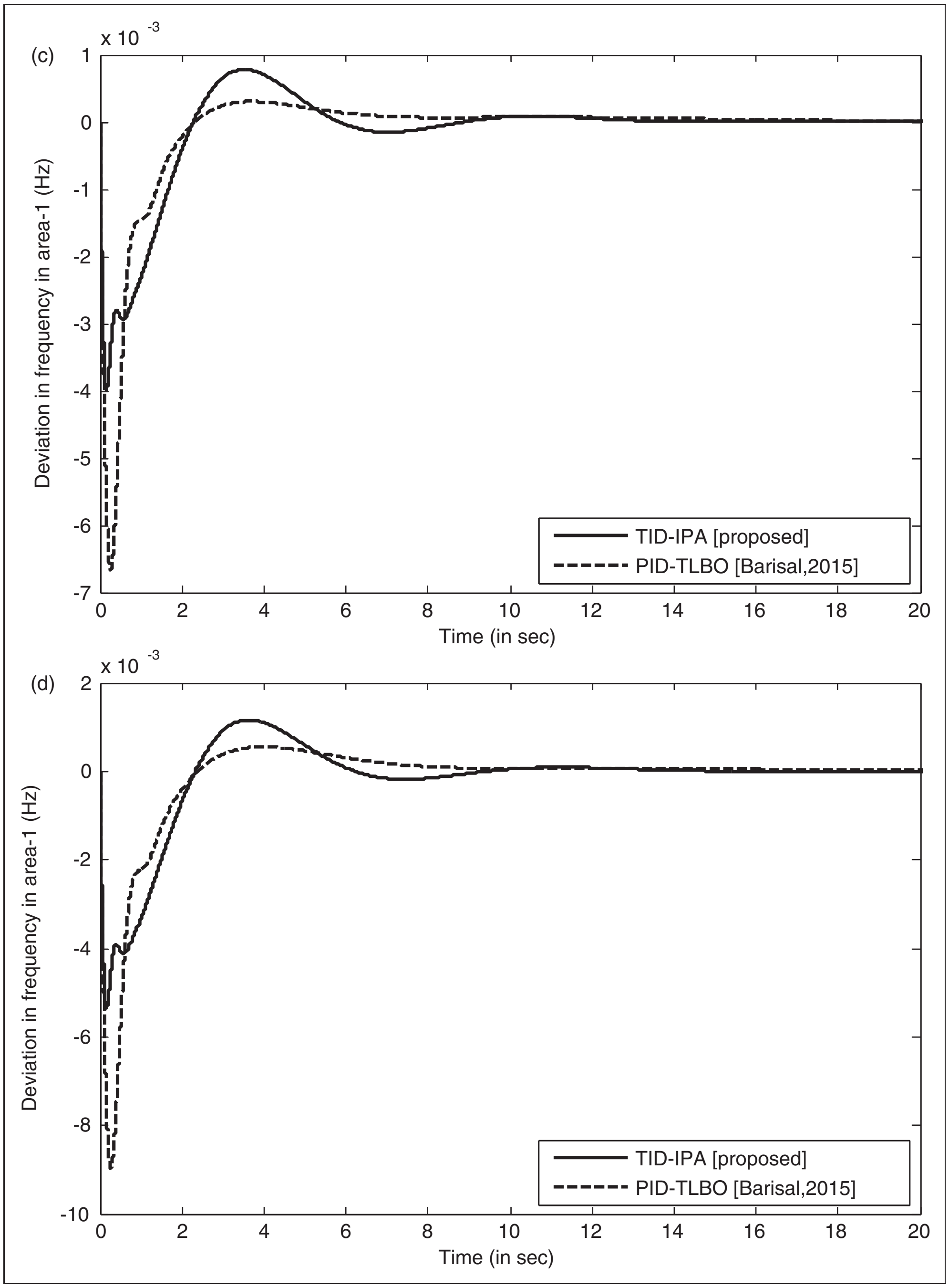


**Figure 5.** Continued.

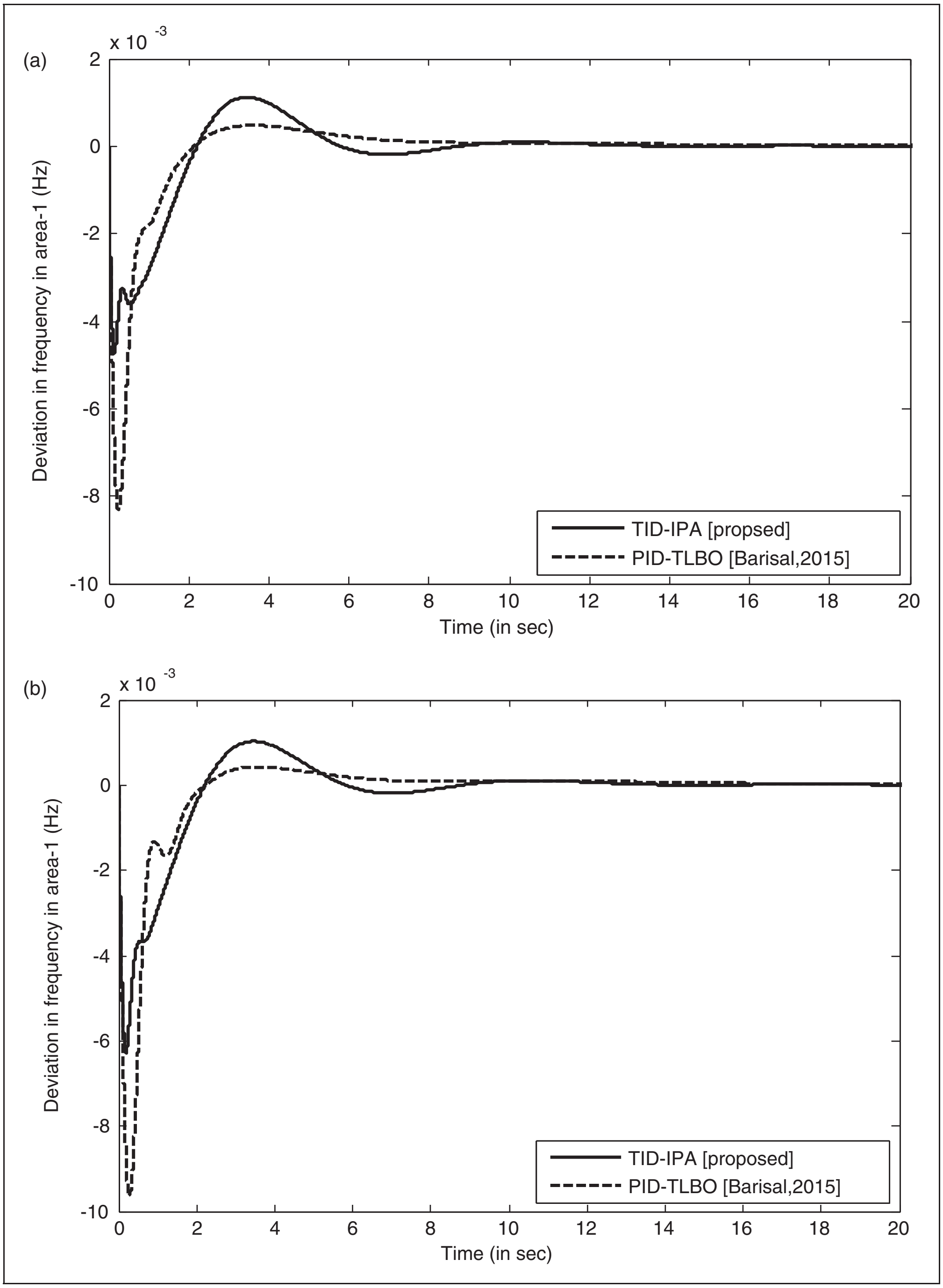


**Figure 6.** (a) Frequency deviation in area-1 due to 50% increase in frequency bias factor. (b) Frequency deviation in area-1 due to 50% increase in constant of turbine. (c) Frequency deviation in area-1 due to 50% increase in operating load condition. (d) Frequency deviation in area-1 due to 50% increase in synchronizing co-efficient. Tilt Integral Derivative Control using Interior Point Algorithm (TID-IPA), Proportional Integral Derivative Control using Teaching Learning Based Optimization (TLBO).

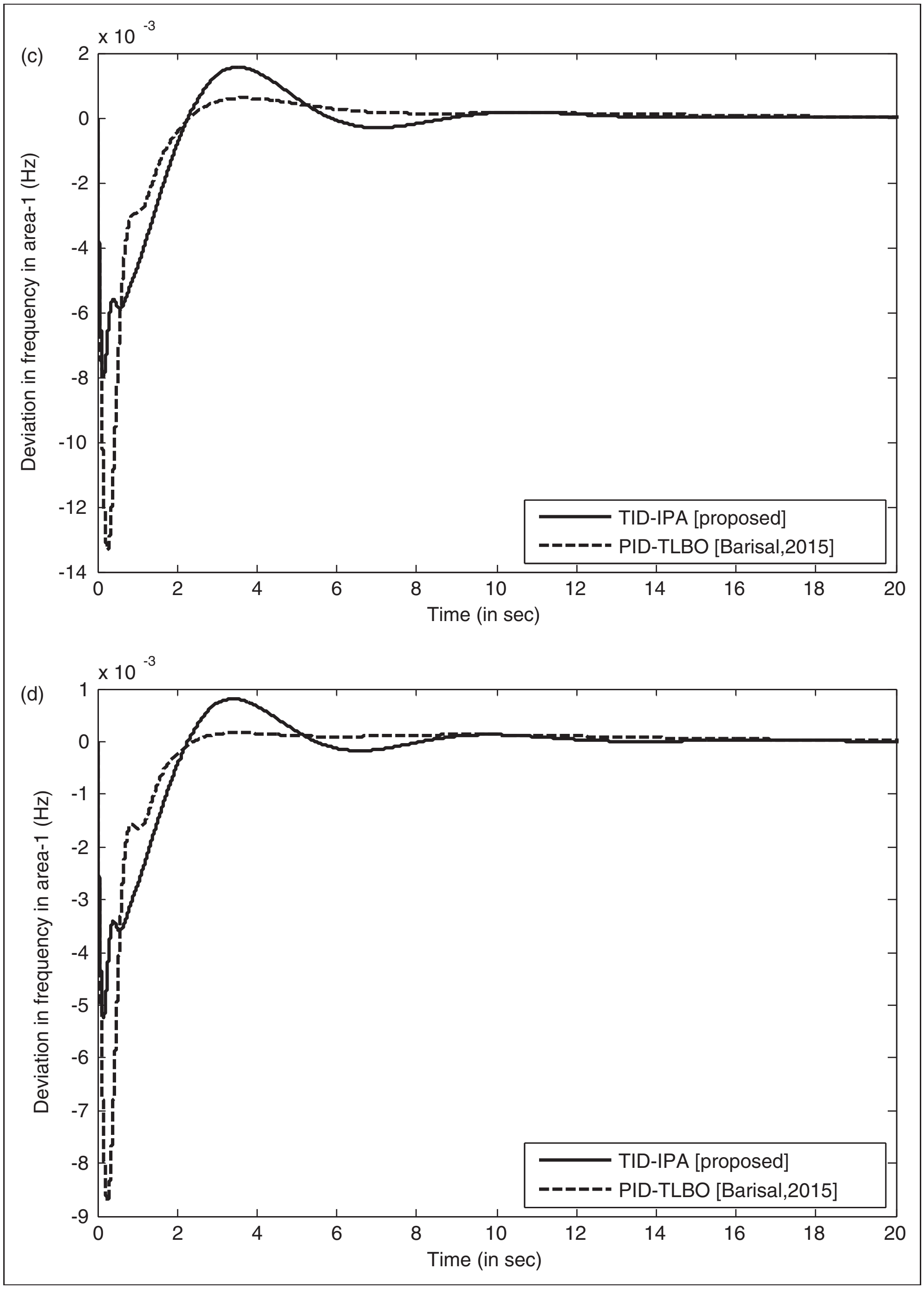


**Figure 6.** Continued.

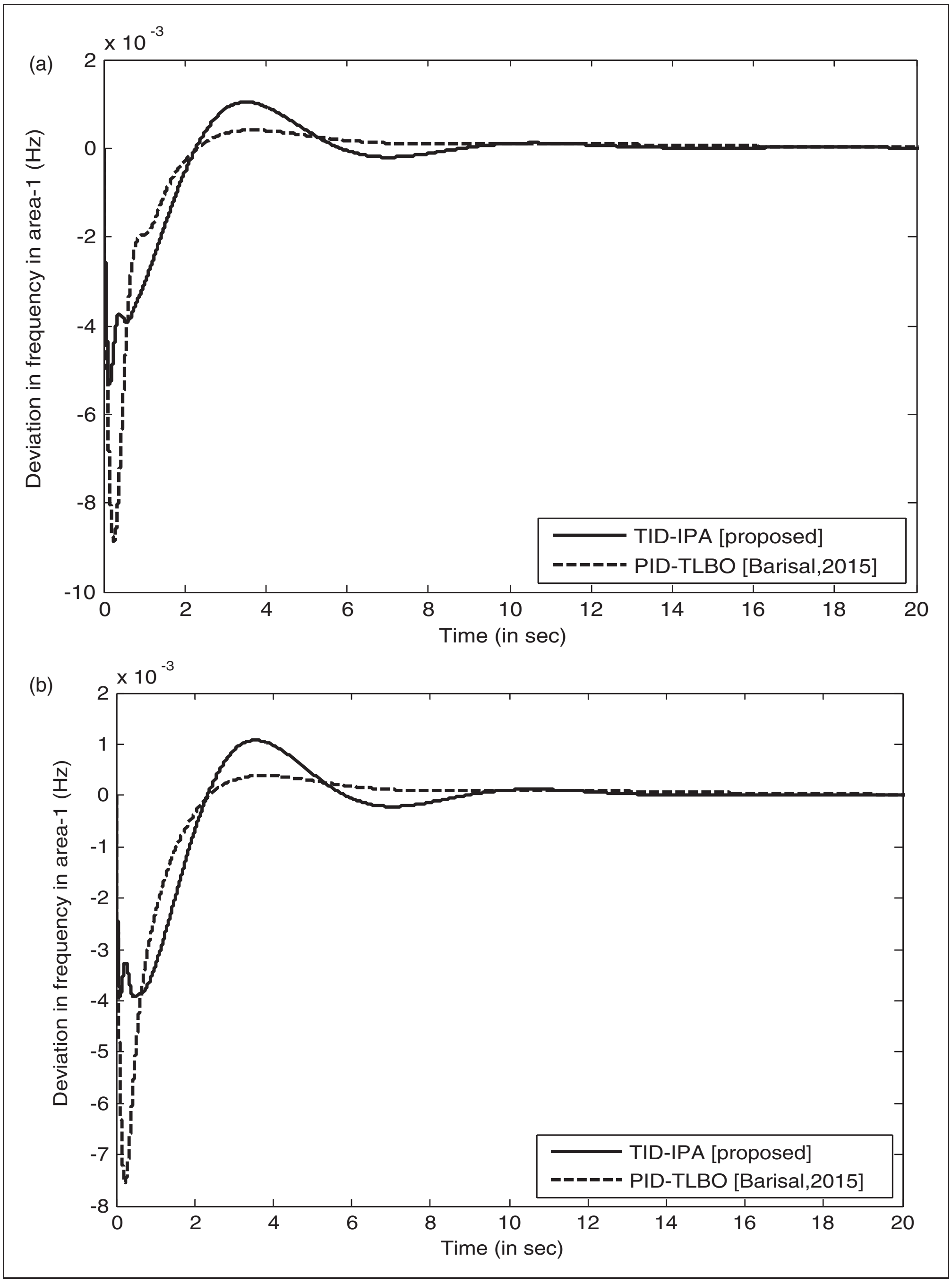


**Figure 7.** (a) Frequency deviation in area-1 due to 50% decrease in frequency bias factor. (b) Frequency deviation in area-1 due to 50% decrease in constant of turbine. (c) Frequency deviation in area-1 due to 50% decrease in operating load condition. (d) Frequency deviation in area-1 due to 50% decrease in synchronizing co-efficient. Tilt Integral Derivative Control using Interior Point Algorithm (TID-IPA), Proportional Integral Derivative Control using Teaching Learning Based Optimization (TLBO).

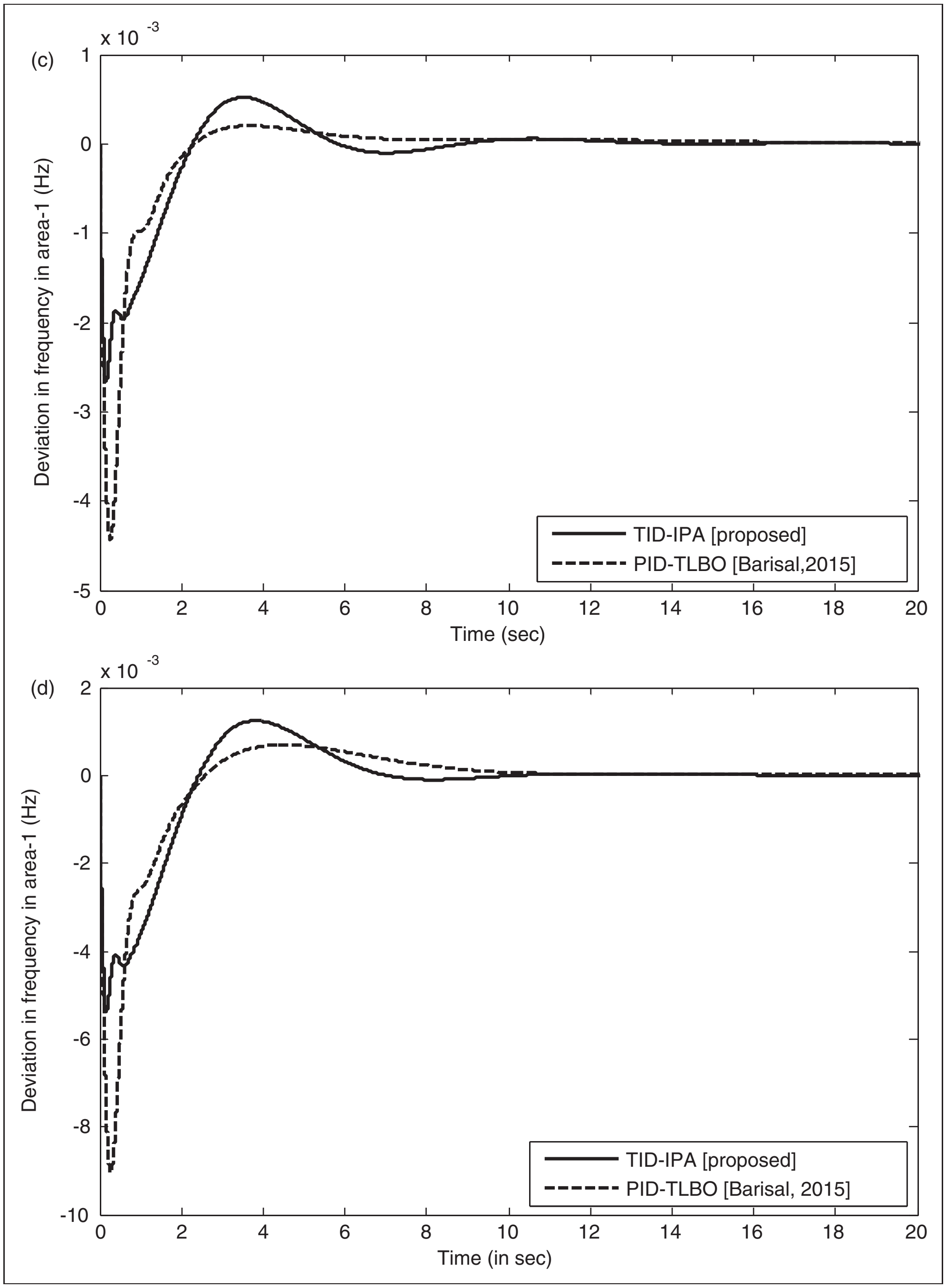


**Figure 7.** Continued.

**Table 1.** Settling time (in sec) and overshoot (in pu) in $\Delta f_1$, $\Delta f_2$ and $\Delta P_{Tie}$ with respect to different controllers at normal operating condition.

| | Controllers | | | |
|---|---|---|---|---|
| | PID controller [Barisal, 2015] | | TID controller [Proposed] | |
| | Settling time | Overshoot | Settling time | Overshoot |
| $\Delta f_1$ | 1.48 | −0.0088 | 0 | −0.0053 |
| $\Delta f_2$ | 0 | −0.0017 | 0 | −0.0016 |
| $\Delta P_{Tie}$ | 0 | −0.0010 | 0 | −0.0009 |

**Table 2.** Value of objective function using different performance indices with respect to PID and TID controller.

| Performance indices | PID controller [Barisal, 2015] | TID controller [Proposed] |
|---|---|---|
| ITAE | 0.10296 | 0.0578 |
| IAE | 0.0163 | 0.0024 |
| ISE | $3.4388 \times 10^{-5}$ | $1.7000 \times 10^{-5}$ |
| ITSE | $2.1972 \times 10^{-5}$ | $1.2921 \times 10^{-5}$ |

which demonstrates that the TID controller has offered a better performance than the PID controller (Barisal, 2015). The system considered was tested through various parameter variations. Some parameters of the system were increased and decreased by 25% and 50% from their nominal value to exhibit wide operating conditions. From the simulation results, it can be concluded that the proposed TID controller is able to provide better performance under various parameter variations than the PID controller (Barisal, 2015).

## Declaration of Conflicting Interests

The author(s) declared no potential conflicts of interest with respect to the research, authorship, and/or publication of this article.

## Funding

The author(s) received no financial support for the research, authorship, and/or publication of this article.

## References

Ai-Hamouz ZM and Abdel-Magid YL (1993) Variable-structure load frequency controllers for multi area power systems. *International Journal of Electric Power and Energy System* 15(5): 23–29.

Aldeen M and Marah JF (1991) Decentralized proportional-plus-integral design method for inter-connected power systems. *IEE Proceedings-C* 138(4): 263–274.

Alomoush MI (2010) Load frequency control and automatic generation control using fractional order controllers. *Journal of Electrical Engineering* 91(7): 357–368.

Barisal AK (2015) Comparative performance analysis of teaching learning based optimization for automatic load frequency control of multi-source power systems. *Electrical Power and Energy Systems* 66: 67–77.

Byrd RH, Hribar ME and Nocedal J (1999) An interior point algorithm for large-scale nonlinear programming. *SIAM Journal on Optimization* 9(4): 877–900.

Cohn N (1967) Considerations in the regulation of interconnected area. *IEEE Transactions on Power Systems* 86: 1527–1538.

Concordia C and Kirchmayer LK (1953) Tie line power and frequency control of electric power systems. *Transactions of the American Institute of Electrical Engineers* 72: 562–572.

Concordia C, Kirchmayer LK and Szymanski EA (1957) Effect of speed governor dead band on tie-line power and frequency control performance. *Transactions of the American Institute of Electrical Engineers Transaction* 76: 429–435.

Debbarma S, Saikia LC and Sinha N (2013) AGC of a multi-area thermal system under deregulated environment using a non-integer controller. *Electric Power Systems Research* 95: 175– 183.

Doolla S and Bhatti TS (2007) A new load frequency control technique for an isolated small hydropower plant. *Proceedings of the Institution of Mechanical Engineers, Part A: Journal of Power and Energy* 221(1): 51–57.

Elgerd OI (1982) *Electric Energy System Theory: An Introduction*, 2nd ed. New York: McGraw-Hill.

Fosha CE and Elgerd OI (1970) The megawatt frequency control problem: a new approach via optimal control theory. *IEEE Transactions on Power Systems* 89: 563–577.

Ghoshal SP (2004) Applications of GA/GASA based fuzzy automatic generation control of a multi- area thermal generating system. *Electric Power Systems Research* 70(2): 115–128.

Gozde H and Taplamacioglu MC (2011) Automatic generation control application with craziness based particle swarm optimization in a thermal power system. *Electrical Power and Energy Systems* 33, pp. 8-16.

Indulkar CS and Raj B (1995) Application of fuzzy controller in automatic generation control. *Electric Machines and Power Systems* 23(2): 209–220.

Kumar A, Malik OP and Hope GS (1985) Variable structure-system control applied to AGC of an interconnected power system. *IEE Proceedings Part C* 132(1): 23–29.

Kundur P (1994) *Power System Stability and Control*. New York: McGraw- Hill.

Kywang YL and El-Sharkawi MA (2008) *Modern Heuristic Optimization Techniques: Theory and Applications to Power Systems*. Hoboken, New Jersey: Wiley-IEEE.

Lurie BJ (1994) Three-parameter tunable tilt-integral derivative (TID) controller. Patent US5371670, USA.

Pan CT and Liaw CM (1989) An adaptive controller for power system load-frequency control. *IEEE Transactions on Power Systems* 14: 122–128.

Parmar KPS, Majhi S and Kothari DP (2012) Load frequency control of a realistic power system with multi-source power generation. *International Journal of Electrical Power and Energy Systems* 42: 426–433.

Podlubny I (1996) Fractional-order systems and $PI^{\lambda}D^{\mu}$-controller. *IEEE Transactions on Automatic Control* 44(1): 208–214.

Pothiya S, Ngamroo I, Runggeratigul S, et al. (2006) Design of optimal fuzzy logic based PI controller using multiple tabu search algorithm for load frequency control. *International Journal of Control, Automation and Systems* 4(2): 155–164.

Ramakrishna KSS and Bhatti TS (2008) Automatic generation control of single area power system with multi-source power generation. *Proceedings of the Institution of Mechanical Engineers, Part A: Journal of Power and Energy* 222(1): 1–11.

Rangaswami D and Sennappan P (2013) Load frequency control using multi-stage fuzzy logic controller for wind-micro hydro-diesel hybrid power system. *Journal of Vibration and Control* 19(7): 1004–1014.

Rerkpreedapong D, Hasanovic A and Feliachi A (2003) Robust load frequency control using genetic algorithms and linear matrix inequalities. *IEEE Transactions on Power Systems* 18(2): 855–861.

Roy R, Bhatt P and Ghoshal SP (2010) Evolutionary computation based three-area automatic generation control. *Expert Systems with Applications* 37(8): 5913–5924.

Shayeghi H, Jalili A and Shayanfar HA (2007) Robust modified GA based multi-stage fuzzy LFC. *Energy Conversion Management* 48(5): 1656–1670.

Sondhi S and Hote YV (2014) Fractional order PID controller for load frequency control. *Energy Conversion Management* 85: 343–353.

Soundarrajan A and Sumathi S (2011) Fuzzy-based intelligent controller for power generating systems. *Journal of Vibration and Control* 17(8): 1265–1278.

Soundarrajan A, Sumathi S and Sivamurugan G (2012) Voltage and frequency control in power generating system using hybrid evolutionary algorithms. *Journal of Vibration and Control* 18(2): 214–227.

Taher SA, Fini MH and Aliabadi SF (2010) Fractional order PID controller design for LFC in electric power systems using imperialist competitive algorithm. *Ain Shams Engineering Journal* 5(1): 121–135.

Tan W (2005) Tuning of PID load frequency controller for power systems. *Electric Power System Research* 50: 1465–1472.

Van Ness JE (1963) Root loci of load frequency control systems. *IEEE Transactions on Power Apparatus and Systems* 82(5): 712–726.

Verma YP and Kumar A (2012) Participation of doubly fed induction generator based wind turbine in frequency regulation with frequency-linked pricing. *Electric Power Components and Systems* 40: 1586–1604.

Waltz RA, Morales JL, Nocedal J, et al. (2006) An interior algorithm for nonlinear optimization that combines line search and trust region steps. *Mathematical Programming* 107(3): 391–408.

Xue D and Chen Y (2002) A comparative introduction of four fractional order controllers. In: *proceedings of the 4th world congress on intelligent control and automation*, Shanghai, P.R. China, 10–12 June, pp.3228-3235.

Xue DY, Zhao C and Chen YQ (2006) Fractional order PID control of A DC-Motor with Elastic Shaft: A Case study. In: *Proceedings of American control conference*, Minneapolis, MN, pp.3182–3187.

Yang TC, Ding ZT and Yu H (2002) Decentralized power system load-frequency control beyond the limit of diagonal dominance. *Electric Power System Research* 24: 173–184.

Zribi M, Al-Rashed M and Alrifai M (2005) Adaptive decentralized load frequency control of multi-area power systems. *Electric Power System Research* 27(8): 575–583.

## Appendix

System parameters: $f = 60$ Hz; B1 = B2 = 0.4312 pu MW/Hz; PR = 2000 MW (rating); PL = 1840 MW (nominal loading); $R_1 = R_2 = R_3 = 2.4$ Hz/pu MW; $T_{sg} = 0.08$ s; $T_r = 10$ s; $K_r = 0.3$; $T_t = 0.3$ s; KT = 0.543478; KH = 0.326084; KG = 0.130438; $T_{gh} = 0.2$ s; $T_{rh} = 28.75$ s; $T_{rs} = 5$ s; $T_W = 1$ s; $b_g = 0.5$; $c_g = 1$; $X_c = 0.6$ s; $Y_c = 1$ s; $T_{cr} = 0.01$ s; $T_{fc} = 0.23$ s; $T_{cd} = 0.2$ s; $T_{ps} = 11.49$ s; $K_{ps} = 68.9566$ Hz/pu MW; $T_{dc} = 0.2$ s; $K_{dc} = 1$; $T_{12} = 0.0433$ pu; a12 = –1.